Energy & Environmental Science

COMMUNICATION

View Article Online
View Journal | View Issue

Cite this: *Energy Environ. Sci.*, 2014, 7, 3600

Received 3rd April 2014
Accepted 15th July 2014

DOI: 10.1039/c4ee01060d

www.rsc.org/ees

Multijunction solar cell efficiencies: effect of spectral window, optical environment and radiative coupling†

Carissa N. Eisler,[a] Ze'ev R. Abrams,[b] Matthew T. Sheldon,[a] Xiang Zhang[bcd] and Harry A. Atwater*[a]

Solar cell efficiency is maximized through multijunction architectures that minimize carrier thermalization and increase absorption. Previous proposals suggest that the maximum efficiency for a finite number of subcells is achieved for designs that optimize for light trapping over radiative coupling. We instead show that structures with radiative coupling and back reflectors for light trapping, *e.g.* spectrum-splitting cells, can achieve higher conversion efficiencies. We model a compatible geometry, the polyhedral specular reflector. We analyze and experimentally verify the effects of spectral window and radiative coupling on voltage and power. Our results indicate that radiative coupling with back reflectors leads to higher efficiencies than previously studied architectures for practical multijunction architectures (*i.e.*, ≤20 subcells).

Broader context

Even with the recent advances in photovoltaics research, 50% solar cell efficiencies have not yet been achieved. Previous designs have focused on a tandem stack structure where semiconductor layers are epitaxially grown or wafer bonded on top of each other, and this presents a significant fabrication challenge. In this design space, the "selective reflector" structure, a design that incorporates reflectors between subcell layers for very strong light trapping, has been identified to be the most efficient theoretical design. However we have identified that spectrum-splitting designs, a class of structures that have not been considered in these kinds of analyses, can give even higher maximum efficiencies and avoid the challenge of stacking multiple bandgap semiconductor layers. This is because some spectrum-splitting geometries can have both strong light trapping and some degree of radiative coupling, or the absorption of radiatively emitted light from a different subcell, owing to the geometry of the structure. We also propose a specific geometry, the polyhedral specular reflector, to have up to 0.6% absolute efficiency increase over the selective reflector design. In our Letter, we extend the understanding of solar cell efficiency and motivate the development of novel spectrum-splitting designs for achieving ultra-high solar efficiencies (>50%).

The photovoltaic community is closer than ever to achieving ultra-high multijunction solar cell efficiencies (>50%).[1–8] Subcells from III–V compound semiconductors are approaching ideal Shockley–Queisser behavior and emit significant radiation of photons with energies equal to or above the optical bandgap because nonradiative recombination has been minimized with advanced growth processes.[6,9] The optical environment of a solar cell controls where the radiated photons from a subcell are directed and this greatly affects its efficiency.[2,3] Thus the optical design of multijunction architectures is crucial for maximizing performance. To date, (1) light trapping and (2) radiative coupling have been investigated as promising optical design strategies. Light trapping inhibits the radiative emission of a subcell in order to reduce the dark current and increase voltage. For example, this can be achieved by including a back reflector on a cell.[9] By contrast, radiative coupling directs radiative emission between neighboring subcells for reconversion.[2,8] Cells that have a high degree of radiative coupling have higher currents and are more tolerant of spectral mismatch because photons can be redistributed and boost carrier generation in the current-limited subcells.[10–15] Thus including both strong light trapping and radiative coupling could yield very high efficiencies. However, only geometries that optimize for either strong light trapping or strong radiative coupling have been considered in the previous literature.[2]

Until now, a proposed structure that only optimizes for light trapping and completely blocks radiative coupling using frequency selective reflectors matched to the band gap emission of each subcell has been assumed to be the most efficient structure for discrete numbers of junctions. This 'selective reflector' design has been shown to give the highest efficiencies for time symmetric structures comprised of a realistic number

[a]*Thomas J. Watson Laboratories of Applied Physics, California Institute of Technology, Pasadena, CA 91125, USA. E-mail: haa@caltech.edu*

[b]*Materials Science Division Lawrence Berkeley National Laboratory, 1 Cyclotron Road, Berkeley, CA 94720, USA*

[c]*Department of Physics, King Abdulaziz University, Jeddah 21589, Saudi Arabia*

[d]*Kavli Energy NanoSciences Institute at the University of California, Berkeley and Lawrence Berkeley National Laboratory, Berkeley, CA 94704, USA*

† Electronic supplementary information (ESI) available. See DOI: 10.1039/c4ee01060d

of junctions (2–20 subcells).[2] Under these same constraints, we instead show here that it is possible to exceed this assumed efficiency limit by incorporating a back reflector for light trapping benefits *and* radiative coupling. Such a design is conceivable with spectrum-splitting architectures whose subcells are mechanically decoupled from one another, for example.[16] Here we investigate different multijunction architectures to provide insight on how their optical environments affect overall efficiencies. We employ a simple model to understand how radiative coupling between subcells with back reflectors can improve multijunction performance and compare this to the previously assumed maximum efficiency case. For cells that do not utilize radiative coupling, we analytically derive and experimentally verify decreases in subcell voltages and efficiencies for architectures that incorporate back reflectors on all subcells. We also show that increasing the radiative coupling between subcells enables these incurred losses to be minimized. Finally, we investigate the effect of radiative coupling between subcells with back reflectors for spectrum-splitting architectures and determine the overall efficiencies for these devices. These efficiencies are also compared to previous idealized geometries and we show where radiative coupling can provide a higher conversion efficiency.

We first review previous time-symmetric multijunction architectures. Fig. 1(a)–(c) show schematics of previously studied cases: the traditional tandem stack, the air-gap tandem stack, and the selective reflector structure.[2] In all of these structures, subcells are stacked in order of decreasing bandgap such that the incident spectrum is divided by above-bandgap absorption of the subcells.[2,3] Both the traditional and air-gap tandem stack structures can radiatively couple between subcells, but the air gap tandem stack can trap some of the radiative emission in the same subcell due to the refractive index contrast at the air–semiconductor interface on both sides of each subcell. By contrast, the selective reflector structure does not have any radiative coupling. The selective reflector is defined to be a mirror with unity reflectivity ($R = 1$) at all photon energies above the energy gap of a given subcell and zero reflectivity ($R = 0$) at all photon energies below the energy gap.[2] This is different from a back reflector that has unity reflectivity at all photon energies and therefore these selective reflector designs have been difficult to realize in practice for monolithic multijunction solar cells. The selective reflector has the same benefit as a back reflector for a given subcell but it can also restrict radiative emission for the next subcell if the difference between bandgaps, or spectral window, is small enough to reflect the radiative emission of the next lowest subcell. Although the air gap tandem structure and the selective reflector structure achieve the same efficiency limit for infinite bandgaps (86.8% for a 6000 K blackbody source), the selective reflector structure is more efficient than the tandem stack structures for finite numbers of subcells because the strong light trapping benefit from the selective reflector greatly outweighs the benefits from radiative coupling in the other structures.[2,13,17,18] However geometries that combine the benefits from a back reflector and radiative coupling can indeed exceed these efficiencies.

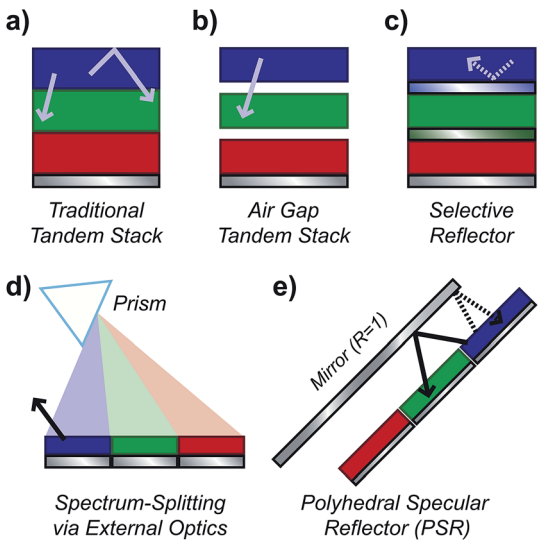

Fig. 1 Schematics of various multijunction cell architectures. Solid arrows denote photons that are radiatively coupled from the blue subcell to the green subcell and dotted arrows denote radiatively emitted photons that are trapped in the same subcell. Structures (a)–(c) represent traditional multijunction architectures that have been studied previously.[2] The selective reflector structure (c) is the most efficient and has no radiative coupling. Structures (d) and (e) represent more novel spectrum-splitting architectures in which subcells are spatially separated from one another. This offers an interesting possibility for radiative coupling between subcells that have their own back reflectors.

Spectrum-splitting geometries have recently regained popularity as multijunction cells begin incorporating more subcells ($\geq$4). Unlike monolithically grown multijunction cells, spectrum-splitting cells can be grown independently of one another, avoiding difficult lattice-matched growth and wafer bonding techniques.[16] In the architectures studied here, light is split and distributed onto a set of independently grown subcells either by an external optical element or by manipulating the packing of the subcells in the structure. We only consider time-symmetric structures to provide the best comparison to the other geometries. A schematic of the spectrum-splitting structure using an external optical element, such as a prism or hologram, is shown in Fig. 1(d).[16,19] This structure allows for back reflectors on each subcell and assumes no radiative coupling between subcells. It will be functionally very similar to the selective reflector structure in the regime where the selective reflector does not restrict radiative emission (*i.e.* $\leq$20 subcells). However, spectrum-splitting structures can exceed the efficiencies of a selective reflector structure if radiatively emitted light can be coupled between subcells that have back reflectors. An example of this is shown in Fig. 1(e) with the polyhedral specular reflector (PSR) design.[16,20–22] Here each subcell, complete with its own back reflector, is placed at a 45° angle in order from the highest to the lowest bandgap opposite a mirror also at 45°. Similar to the multijunction designs in Fig. 1(a)–(c), incident light is split by above bandgap absorption but in this design, light that is not absorbed is directed to the next subcell *via* specular reflections off of the back reflector and opposing mirror. The PSR is particularly interesting because light trapping and radiative coupling are inherent to the geometry, shown by the rays in Fig. 1(e). The solid ray shows a radiatively emitted photon that is downshifted to the next subcell and the dotted ray shows a radiatively emitted

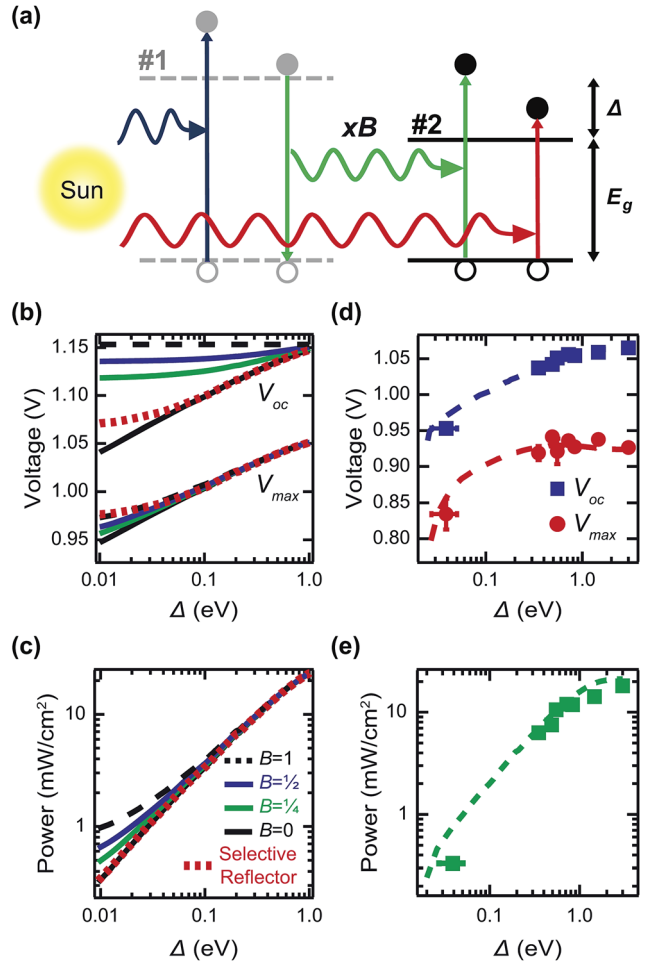

Fig. 2 (a) Band energy diagram and schematic of the two subcell model. Subcell #2 can absorb solar photons from its input spectral window (red) or photons produced *via* radiative recombination in subcell #1 (green). (b)–(c) Theoretical light *I*–*V* subcell characteristics as a function of spectral window, Δ, for a subcell with $E_g = 1.42$ eV (*e.g.* GaAs) for $B = 0$, 1/4, 1/2 and 1. Radiative coupling strongly affects the subcell (b) voltage and (c) power for small values of Δ. (d)–(e) Experimental verification of light *I*–*V* characteristics for a GaAs subcell with no absorbed radiation from another cell (*i.e.* $B = 0$). The (d) measured voltages V_{oc} and V_{max} and the (e) measured subcell power (markers) closely follow the modeled response (dashed lines).

photon that is reflected back onto the same subcell. Because this geometry can recycle radiatively emitted photons between subcells that have back reflectors, we derive a higher conversion efficiency beyond that in previously studied geometries.

We simplify the analysis of radiative coupling to a two subcell system in which a higher bandgap subcell radiatively couples to a lower bandgap subcell. This provides a starting point for modeling optical interactions in a multijunction cell where all subcells are independently connected and have their own back reflectors. A band diagram and schematic of the two subcell model is shown in Fig. 2(a). Subcell #2, the subcell of interest, has a bandgap of E_g and subcell #1, the source of radiated photons, has a bandgap of $E_g + \Delta$. Both subcells are assumed to be ideal semiconductors that absorb all photons with energies above their respective bandgaps. Subcell #1 receives all photons above its bandgap from the input spectra while subcell #2 is limited to a narrow spectral window, Δ, of the input spectrum. We qualitatively relate Δ to the number of subcells in a hypothetical multijunction cell because adding more subcells to a structure decreases the spectral window on each subcell. For simplicity, we assume that the only radiative coupling mechanism is subcell #2 absorbing photons emitted from subcell #1.

We then define a geometric parameter B to describe the radiative coupling from subcell #1 to subcell #2. B represents the fraction of radiatively emitted photons directed from subcell #1 to #2 such that $0 \leq B \leq 1$, analogous to the down converting literature, and is determined by the optical architecture of the multijunction cell.[23,24] $B = 1$ is time-asymmetric because radiative emission is completely downshifted and does not obey absorption–emission symmetry, but we include it in our analysis as an upper limit to this downshifting system.[3,4,25] The specific structures we study here have varying degrees of radiative coupling but are still time-symmetric. For example, the traditional tandem stack (Fig. 1(a)) would have a B of ~0.93–0.98 because radiatively emitted photons are reflected at the front air–semiconductor interface (large index of refraction contrast) and transmitted through the rear semiconductor–semiconductor interface to the bottom subcell (little to no index contrast).[14] The air gap tandem stack (Fig. 1(b)) has a smaller B of 0.5 because there is an air–semiconductor interface on both sides and so radiation is emitted equally on both faces. The generic spectrum-splitting structure of Fig. 1(d) corresponds to $B = 0$ because its subcells are optically independent. However not all spectrum-splitting structures are optically isolated. For example, the PSR (Fig. 1(e)) has some radiative coupling ($B = 0.204$) because some of the radiated photons will reflect off of the mirror and onto the next subcell in line. Although the subcells are not directly in optical contact as in the tandem stack structure, radiatively emitted photons can still be coupled between independently connected subcells.

Assuming the subcells in the simplified system are characterized under the 1 sun AM1.5D spectrum and have a front air interface, we can calculate the power produced in subcell #2 as a function of B and Δ using basic detailed balance principles.[26,27] See the ESI† material for the full derivation. The power produced in subcell #2 is given by:

$$P_2 = V_2 J_2 = V_2 \left[\int_{E_g}^{E_g+\Delta} N_{AM1.5D}(E)\mathrm{d}E + \frac{2\pi q}{h^3 c^2} \left(B \int_{E_g+\Delta}^{\infty} \frac{E^2 \mathrm{d}E}{\exp\left(\frac{E - qV_1}{kT_o}\right) - 1} - \int_{E_g}^{\infty} \frac{E^2 \mathrm{d}E}{\exp\left(\frac{E - qV_2}{kT_o}\right) - 1} \right) \right]$$

where V is the operating voltage of a subcell, J is the current produced in a subcell, $N_{AM1.5D}$ is the photon flux as a function of energy in the 1 sun AM1.5D spectrum, q is the charge of an electron, h is Planck's constant, c is the speed of light, k is Boltzmann's constant, and T_o is the temperature of the subcell (300 K). The current in subcell #2 has three important contributions: current produced from the input spectra, current produced from reconverting radiated photons from subcell #1, and the dark current resulting from radiating photons.

We investigate the open-circuit ($V_{oc,2}$) and maximum power voltage ($V_{max,2}$) conditions for subcell #2. Open circuit voltage ($V_{oc,2}$) occurs when the radiative current exactly balances the photogenerated current while the maximum power voltage ($V_{max,2}$) refers to the voltage when the power is maximized.† [28–30] Under both conditions, voltage increases when the current for subcell #2 increases, which is caused by an increased number of incident photons. For the same value of Δ, a higher B will yield a higher current and therefore a higher voltage. $V_{oc,2}$ and $V_{max,2}$ are plotted in Fig. 2(b) for an example bandgap of $E_g = 1.42$. Both voltage conditions show a decline with decreasing Δ resulting from subcell #2 receiving fewer photons under the restricted spectrum and this decline is lessened with a higher value of B. The only exception to this trend is when $B = 1$ for $V_{oc,2}$. When $B = 1$, all photons absorbed into subcell #1 are downshifted to subcell #2 and $V_{oc,2}$ equals the V_{oc} of the subcell operating as a single junction cell having full access to the entire input spectrum regardless of the value of Δ.† [26,30] We plot these with the voltages for a two subcell selective reflector structure (dotted red) whose derivation can be found elsewhere.† [2] Both the $V_{oc,2}$ and the $V_{max,2}$ of a subcell with selective reflectors closely follow the $B = 0$ case until $\Delta \leq 0.6$ eV when the curves begin declining much less rapidly, similar to $B > 0$. Until $\Delta \leq 0.6$ eV, the spectral window is wide enough that the selective reflector does not restrict any of the radiative emission and so it only acts as a back reflector. Therefore these trends match the voltages of the $B = 0$ case. Only when this curve diverges does the selective reflector subcell has an advantage in voltage over radiative coupling subcells.

We also study the maximum power (P_2) for subcell #2 in Fig. 2(c). Similar to the voltage, the maximum power decreases monotonically with Δ because a reduced photon flux will decrease both photocurrent and voltage. This decline is still the most severe for $B = 0$ because there is no radiative coupling to compensate for a smaller spectral window. The inclusion of radiative coupling ($B > 0$) lessens the decline in maximum power due to additional photocurrent. Unlike the previously studied voltage conditions, the power generated in the selective reflector case closely follows the $B = 0$ curve even beyond $\Delta \leq 0.6$ eV. Restricting the emission of a subcell can increase its voltage, but the additional current from radiative coupling in the $B > 0$ cases is more advantageous. However, we recognize that the improvement for the $B > 0$ cases here may be exaggerated due to only studying radiative coupling between two absorbers and so we study full multijunction ensembles later on.

To verify the theory discussed, we measured the light I–V characteristics of a high quality GaAs solar cell in the absence of radiative coupling ($B = 0$).[6,9] The current–voltage response of the cell was characterized by a solar simulator under 100 mW cm^{-2} of AM1.5 G illumination. The spectral window was adjusted using longpass filters that act as subcell #1 and block photons with wavelengths shorter than the filter cutoff wavelength. Fig. 2(d) and (e) show the dependence of the experimental V_{oc}, V_{max}, and maximum power on the available spectrum in the absence of radiative coupling. The above expressions are modified to incorporate realistic device losses for comparison to the experimental devices.† [3,6,31] Fig. 2(d) and (e) show an excellent correspondence of the data to our model. All three parameters, V_{oc}, V_{max}, and P_{max}, show a significant decline with decreasing spectral windows.

We now extend our analysis of radiative coupling to full multijunction devices. We calculated the efficiencies for ideal multijunction cells with 2 to 20 subcells under the 1 sun AM1.5D G173-03 spectrum. The bandgaps for each ensemble were determined by detailed balance optimizations discussed elsewhere.† [32] The efficiencies are calculated for the cases illustrated in Fig. 1 as well as some additional cases from our study ($B = 0$, 1/4, 1/2, and 1) for reference.[2] All cases with radiative coupling assume that absorption of radiatively emitted photons only occurs when the absorbing subcell has a smaller bandgap than the emitting subcell. This assumption is valid for this range of subcells because the vast majority of radiatively emitted photons from a given subcell have too small of an energy to be converted by a subcell with a higher bandgap. For the PSR, we assume that 20.2% of photons are downshifted, 20.7–41.4% of photons are reflected back into the same subcell (depending on the subcell position), and that the remaining photons are lost.† There is a concentration factor of $1/\sqrt{2}$ owing to the geometry of the structure.† We also only assume radiative coupling between adjacent subcells of the PSR for simplicity.

Fig. 3 shows efficiency as a function of the number of subcells for these cases. We show that a traditional tandem stack is less efficient than the air gap structure. Although there is a higher radiative coupling for the traditional tandem stack ($B > 0.9$), there is increased light trapping in the air gap structure and so the air gap tandem stack has smaller dark currents and a higher overall efficiency. We also verify previous literature by showing that the selective reflector case is more efficient than the traditional and air gap tandem stack cases because the selective reflectors increase light trapping by providing the benefits of a back reflector. In contrast to previous literature, we show that structures with radiative coupling and back reflectors ($B > 0$, PSR) are the most efficient for 2–20 subcells. For low numbers of subcells (<20), the selective reflectors only act as back reflectors and do not restrict emission because the spectral windows encompass the majority of the radiatively emitted photons. Essentially all radiatively emitted photons in the selective reflector case escape the multijunction cell without being recycled and so the dark current is not significantly reduced. This is further corroborated by the fact that the efficiencies for this case are equivalent to our case with no radiative coupling (spectrum-splitting *via* external optics, $B = 0$), which we have also identified as the worst case in our previous model. By contrast, radiative coupling ($B > 0$) allows these photons to be reconverted, thus boosting the current in lower bandgap

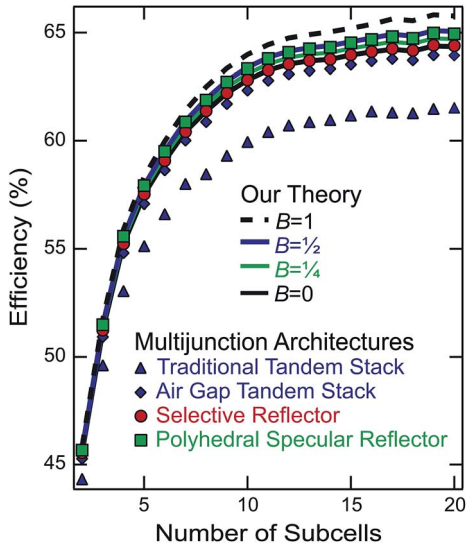

Fig. 3 Theoretical efficiencies for multijunction ensembles as a function of the number of subcells. Varying amounts of radiative coupling with back reflectors ($B = 0$, 1/4, 1/2, 1) are compared to the traditional tandem stack (blue triangles), air gap tandem stack (blue diamonds), selective reflector (red circles), and polyhedral specular reflector (green squares) geometries under the 1 sun AM1.5D spectrum. The polyhedral specular reflector is shown to be more efficient than the previous maximum efficiency case (selective reflector).

subcells and providing higher efficiencies (up to 1.5% absolute increase) than the selective reflector case, as shown in Fig. 3. Even the PSR design, which has a concentration <1 because of its geometry, outperforms the selective reflector case because radiatively emitted photons can be recycled within the same subcell and coupled among other subcells. This combined light trapping and radiative coupling also explains why the structure performs closely to the example $B = 1/2$ case even though in this case B is less than 1/4. Thus a spectrum-splitting design that incorporates back reflectors for each subcell with radiative coupling between subcells and/or light trapping could provide a significant increase in efficiency over previously studied designs.[16,21,22,33,34]

Our analysis and experimental results show the important role of radiative coupling and how spectral window and optical environment dictate the performance of subcells in a multijunction cell. As the number of subcells increases, the photon flux each subcell receives will decrease, reducing the power it converts, and this dependence is exacerbated when there is a lack of photon recycling between subcells. However, if subcells can radiatively couple into other subcells, this reduction is less significant. Additionally, we studied maximum efficiencies of multijunction ensembles and have shown that for 2–20 subcells, even higher efficiencies can be obtained than what was previously thought possible by including both radiative coupling between subcells and a back reflector on each subcell, as exemplified here by the PSR geometry. Therefore spectrum-splitting designs that allow for radiative coupling between subcells and have back reflectors on every subcell will lead the next generations of ultra-high efficiency multijunction cells.

Experimental

Alta Devices provided thin-film, flexible GaAs solar cells for the experimental portion of this study. The light I–V response of the cell was measured under 100 mW cm^{-2} of simulated AM1.5 G illumination using a Keithley 238 high current source measure unit. A longpass filter was placed above the cell to block higher energy photons in the input spectrum, varying the spectral width. The filters used blocked wavelengths shorter than 430 nm (Chroma ET430lp), 550 nm (Newport 10LWF-550-B), 580 nm (Chroma HQ580lp), 630 nm (Chroma HQ630lp), 650 nm (Thorlabs FEL650), 700 nm (Thorlabs FEL700), and 850 nm (Thorlabs 850 nm).

Acknowledgements

This work is part of the 'Light–Material Interactions in Energy Conversion' Energy Frontier Research Center funded by the U.S. Department of Energy, Office of Science, Office of Basic Energy Sciences under Award Number DE-SC0001293. C. N. Eisler was supported by the Department of Defense (DoD) through the National Defense Science & Engineering Graduate Fellowship (NDSEG) Program. The authors wish to thank E. Kosten and E. Warmann for invaluable discussion as well as B. Kayes and Alta Devices for providing the GaAs cells used in this study.

References

1 C. H. Henry, *J. Appl. Phys.*, 1980, **51**, 4494–4500.
2 A. Martí and G. L. Araújo, *Sol. Energy Mater. Sol. Cells*, 1996, **43**, 203–222.
3 M. A. Green, in *Third Generation Photovoltaics: Advanced Solar Energy Conversion*, ed. Kamiya T, Monemar B, Venghaus H and Yamamoto Y, Springer-Verlag, Berlin, Heidelberg, 2003, ch. 5, pp. 59–69.
4 A. S. Brown, Ph.D. thesis, University of New South Wales, 2003.
5 R. R. King, A. Boca, W. Hong, X.-Q. Liu, D. Bhusari, D. Larrabee, K. M. Edmonson, D. C. Law, C. M. Fetzer, S. Mesropian, N. H. Karam, *24th European Photovoltaic Solar Energy Conference and Exhibition*, Hamburg, Germany, 2009.
6 M. A. Green, *Prog. Photovolt. Res. Appl.*, 2012, **20**, 472–476.
7 A. Polman and H. A. Atwater, *Nat. Mater.*, 2012, **11**, 174–177.
8 M. A. Green, K. Emery, Y. Hishikawa, W. Warta and E. D. Dunlop, *Prog. Photovolt. Res. Appl.*, 2013, **21**, 1–11.
9 O. D. Miller, E. Yablonovitch and S. R. Kurtz, *IEEE Journal of Photovoltaics*, 2012, **2**, 303.
10 C. Baur, M. Hermle, F. Dimroth and A. W. Bett, *Appl. Phys. Lett.*, 2007, **90**, 192109.
11 M. A. Steiner, J. F. Geisz, T. E. Moriarty, R. M. France, W. E. McMahon, J. M. Olson, S. R. Kurtz and D. J. Friedman, *IEEE Journal of Photovoltaics*, 2012, 1–9.
12 M. A. Steiner and J. F. Geisz, *Appl. Phys. Lett.*, 2012, **100**, 251106.
13 G. L. Araujo, A. Marti, *Conference Record of the Twenty Second IEEE Photovoltaics Specialists Conference*, 1991.

14 D. J. Friedman, J. F. Geisz and M. A. Steiner, *IEEE Journal of Photovoltaics*, 2013, **3**, 1429–1436.
15 A. S. Brown and M. A. Green, *Conference Record of the Twenty-Ninth IEEE Photovoltaic Specialists Conference*, New Orleans, LA, 2002, pp. 868–871.
16 A. G. Imenes and D. R. Mills, *Sol. Energy Mater. Sol. Cells*, 2004, **84**, 19–69.
17 A. De Vos, *J. Phys. D: Appl. Phys.*, 1980, **13**, 839–846.
18 A. De Vos, in *Thermodynamics of Solar Energy Conversion*, Wiley-VCH, Verlag, Weinheim, 2008.
19 M. Escarra, S. Darbe, E. C. Warmann and H. A. Atwater, *Conference Record of the Thirty-Ninth IEEE Photovoltaic Specialists Conference*, Tampa, FL, 2013.
20 E. M. Ellion, *World Pat.*, 8,701,512, 1987.
21 B. Mitchell, G. Peharz, G. Siefer, M. Peters, T. Gandy, J. C. Goldschmidt, J. Benick, S. W. Glunz, A. W. Bett and F. Dimroth, *Prog. Photovoltaics*, 2011, **19**, 61–72.
22 C. N. Eisler, E. D. Kosten, E. C. Warmann and H. A. Atwater, *Conference Record of the Thirty-Ninth IEEE Photovoltaic Specialists Conference*, Tampa, FL, 2013.
23 V. Badescu, A. De Vos, A. M. Badescu and A. Szymanska, *J. Phys. D: Appl. Phys.*, 2007, **40**, 341–352.
24 Z. R. Abrams, A. Niv and X. Zhang, *J. Appl. Phys.*, 2011, **109**, 114905.
25 M. A. Green, *Nano Lett.*, 2012, **12**, 5985–5988.
26 W. Shockley and H. J. Queisser, *J. Appl. Phys.*, 1961, **32**, 510.
27 M. A. Green, *Prog. Photovoltaics*, 2012, **20**, 127–134.
28 A. De Vos and H. Pauwels, *Appl. Phys. A: Mater. Sci. Process.*, 1981, **25**, 119–125.
29 R. T. Ross, *J. Chem. Phys.*, 1967, **46**, 4590–4593.
30 W. Ruppel and P. Wurfel, *IEEE Trans. Electron Devices*, 1980, **27**, 877–882.
31 J. L. Gray, in *Handbook of Photovoltaic Science and Engineering*, ed. Luque, A. and Hegedus, S., John Wiley & Sons, West Sussex, United Kingdom, 2003, ch. 3, pp. 102–104.
32 E. C. Warmann, C. N. Eisler, E. D. Kosten, M. Escarra and H. A. Atwater, *Conference Record of the Thirty-Ninth IEEE Photovoltaic Specialists Conference*, Tampa, FL, 2013.
33 U. Ortabasi, A. Lewandowski, R. McConnell, D. J. Aiken, P. L. Sharps and B. G. Bovard, *Conference Record of the Twenty-Ninth IEEE Photovoltaic Specialists Conference*, New Orleans, LA, 2002, pp. 1616–1620.
34 E. D. Kosten, J. Lloyd, E. C. Warmann and H. A. Atwater, *Conference Record of the Thirty-Ninth IEEE Photovoltaic Specialists Conference*, Tampa, FL, 2013.